BLOCK-ORIENTED GRAY BOX MODELING OF GUITAR AMPLIFIERS

Felix Eichas, Stephan Möller, Udo Zölzer

Department of Signal Processing and Communications,
Helmut Schmidt University
Hamburg, Germany
felix.eichas@hsu-hh.de

ABSTRACT

In this work, analog guitar amplifiers are modeled with an automated procedure using iterative optimization techniques. The digital model is divided into functional blocks, consisting of linear-time-invariant (LTI) filters and nonlinear blocks with nonlinear mapping functions and memory. The model is adapted in several steps. First the filters are measured and afterwards the parameters of the digital model are adapted for different input signals to minimize the error between itself and the analog reference system. This is done for a small number of analog reference devices. Afterwards the adapted model is evaluated with objective scores and a listening test is performed to rate the quality of the adapted models.

1. INTRODUCTION

Musical distortion circuits, especially guitar amplifiers, have been the subject of virtual analog modeling for years. There exist two main modeling approaches, like white-box modeling and black- or gray-box modeling. White-box modeling makes use of everything known about the reference system, for example its circuit and the characteristics of the circuit elements. In [1–3] the circuit of each reference is modeled by creating a (nonlinear) state-space model. To be able to do that, detailed knowledge about the circuit diagram as well as the nonlinear characteristics of the circuit elements is required. In [4] an alternative white-box modeling approach is described, where wave digital filters are used to model the circuit of a reference device. This approach has already been used in [5] to model a guitar pre-amplifier with four vacuum triodes and a complex circuit topology. Both white-box approaches give very good results which can reproduce all relevant characteristics of a reference device. If the sound of a specific analog device should be replicated with high accuracy, the white-box modeling approaches are preferable. The drawback of both approaches is the computational load of the model. Without simplifications and pre-calculations, the model of a circuit with complex topology and a lot of nonlinear elements will barely be real-time capable.

In [6] a distortion circuit for electric guitars is modeled with a gray-box modeling approach. The reference system is measured with an exponential sine sweep, which allows to construct a multi-branch Hammerstein model where each branch represents a harmonic oscillation of the fundamental frequency of the input signal. Each branch is then filtered with the corresponding filter obtained with the exponential sine sweep analysis. This method gives good results, but the polynomials used as nonlinear mapping curves in each branch of the model are amplitude dependent, which means that the model gives perfect results if the input signal has the same amplitude as the identification signal, but might not perform as well for other amplitudes.

This work describes a gray-box modeling approach, which is similar to [6], but with a different model structure and iterative optimization to adjust the parameters of the digital model. The only assumptions made about the reference system are its basic structure. The modeling procedure is completely automatic and uses solely input-output measurements and iterative optimization to adapt the digital model to the reference device. No knowledge about the circuit is required.

System identification or modeling approaches are already used in commercial products. In [7] the modeling procedure is not automated and it becomes obvious that it is a quite tedious process. The patent [8] details a gray box modeling approach for guitar amplifiers. A Wiener-Hammerstein model is used, consisting of an input filter in series with a memoryless nonlinearity and an output filter. In the patent the modeling process is detailed only vaguely, for example, the mathematical basis for the nonlinear mapping function is not explained. Nevertheless, the results of this method speak for themselves, since a lot of musicians already use the commercial product, because of its flexibility in sound design.

One major drawback of the gray-box modeling techniques is, that the user controls (e.g. knobs on the amplifier) can not be modeled without creating one model for every possible combination of user controls and then interpolate between the model's parameters, according to the current user control setting.

This work describes the structure of the proposed digital model in Section 2. Section 3 details the measurement setup which is used to measure all guitar amplifiers. Sections 4 and 5 explain the steps used to adapt the model with the iterative optimization routine and show objective and subjective results. In Section 6 conclusions are drawn.

2. DIGITAL MODEL

The overall structure of the digital model is straightforward and has been used in virtual analog modeling before. The model consists of linear-time-invariant (LTI) blocks and nonlinear blocks which introduce harmonic distortion. In [7] this structure has been described as 'the fundamental principle of guitar tone', since every guitar-specific audio system, regardless if it is an analog or a digital system, operates in this manner. As Fig. 1 depicts, the input signal is filtered by the first filter, afterwards it is distorted by the first nonlinear block, which corresponds to the nonlinear behavior of the pre-amplifier. The output of the pre-amplifier is then filtered by the next filter in the cascade, which corresponds to the tone-section of the guitar amplifier. Finally, the signal passes through the second nonlinear block, corresponding to the power stage of the guitar amplifier and is then filtered by the output filter. The first filter in an analog amplifier are mostly first order RC-highpass or RC-bandpass filters and the output filter is determined

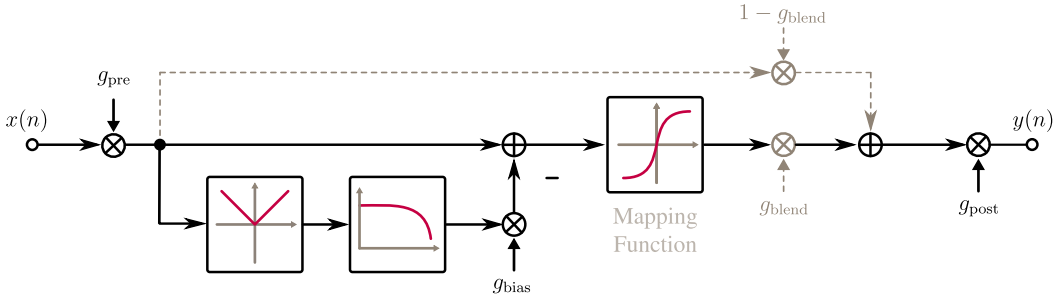

Figure 2: *Signal flow graph of a nonlinear block. Blend stage is omitted in the second nonlinear block.*

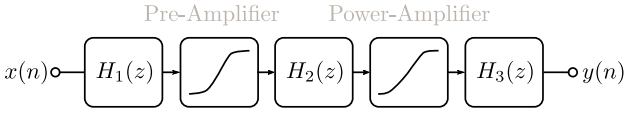

Figure 1: *Block diagram of a guitar amplifier and structure of the digital model.*

by the frequency behavior of the output transformer.

For analog guitar amplifiers, the distinction between the blocks is not always this clear. For example many amplifiers are designed in such a way, that turning the drive- or gain-knob down, the frequency response of the input filter is also changed.

Please note that the last filter $H_3(z)$ does not correspond to the impulse response of a loudspeaker. The amplifiers were measured without the influence of any speaker.

2.1. Pre-Amplifier Nonlinearity

All nonlinear blocks are structured as depicted in Fig. 2. This nonlinear block originated from [9] and has already been used in distortion effect modeling. The most important part of each nonlinear block is the mapping function because it defines the spectral shape of the harmonics.

The first nonlinear block consists of a polynomial mapping function which is complemented with pre- and post-gains, as well as a blend parameter, allowing dry/wet mixing of the output signal. The advantage of polynomial wave-shaping functions is the mathematical relationship between the coefficients of the polynomial and the shape of the harmonic overtones in the spectrum. Consider a polynomial function,

$$p(x) = a_0 + a_1 x + a_2 x^2 + \ldots + a_N x^N, \qquad (1)$$

where x is the input variable (corresponding to the amplitude of the input signal) and a_n with $n \in [0, N]$ are the coefficients of the polynomial. Substituting x with $\tilde{x} = u \cdot \cos(\omega t)$, it is possible to separate the different harmonic oscillations of the fundamental frequency,

$$p(\omega t) = k_0 + k_1 \cos(\omega t) + k_2 \cos(2\omega t) + \ldots + k_N \cos(N\omega t), \quad (2)$$

where the variables a_n and u have been combined into the harmonic variables k_n. Each k_n describes the amplitude of the n-th harmonic to the fundamental frequency f_0 or ω_0 for a fixed input amplitude u. Fig. 3 depicts the harmonic variables k_n in frequency domain.

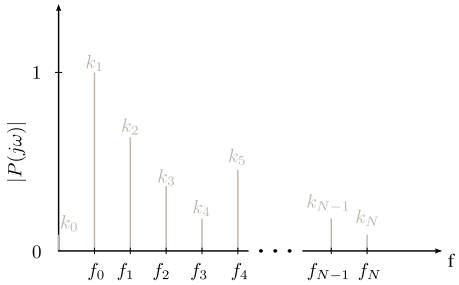

Figure 3: *Overtones of a sinusoidal signal after the polynomial mapping function.*

The relationship between harmonic variables k_n and polynomial coefficients a_n can be written in matrix form,

$$\begin{pmatrix} A_{11} & A_{12} & \ldots & A_{1N} \\ A_{21} & A_{22} & \ldots & A_{2N} \\ A_{31} & A_{32} & \ldots & A_{3N} \\ \vdots & \vdots & \ddots & \vdots \\ A_{N1} & A_{N2} & \ldots & A_{NN} \end{pmatrix} \begin{pmatrix} a_0 \\ a_1 \\ a_2 \\ \vdots \\ a_N \end{pmatrix} = \begin{pmatrix} k_0 \\ k_1 \\ k_2 \\ \vdots \\ k_N \end{pmatrix}$$

and solved for every a_n. With this technique it is possible to calculate the polynomial mapping function which creates the desired shape of overtones.

As an example the matrix equation is shown for 4 harmonics.

$$\begin{pmatrix} 1 & 0 & u^2/2 & 0 & 3u^4/8 \\ 0 & u & 0 & 3u^3/4 & 0 \\ 0 & 0 & 0 & u^3/4 & 0 \\ 0 & 0 & 0 & 0 & u^4/8 \end{pmatrix} \begin{pmatrix} a_0 \\ a_1 \\ a_2 \\ a_3 \\ a_4 \end{pmatrix} = \begin{pmatrix} k_0 \\ k_1 \\ k_2 \\ k_3 \\ k_4 \end{pmatrix}$$

Another extension, which has been made to the nonlinear blocks of the model, has been proposed in [10]. The envelope of the input signal is calculated and added to the signal, directly before the nonlinear mapping function. This behavior simulates the signal-dependent bias-point shift that is happening in tube amplifiers due to a varying cathode voltage which alters the plate current and thus moving the bias point of the tube.

2.2. Power-Amplifier Nonlinearity

The nonlinear block of the digital model, corresponding to the power stage of the guitar amplifier is slightly different than the first nonlinear block. Instead of using a polynomial mapping function, a concatenation of three hyperbolic tangents is used, which allows to shape positive and negative half-waves separately. It was already used in [9,11] to model distortion audio circuits. The blend stage was omitted in this nonlinear block.

3. MEASUREMENT SETUP

In this work, all measurements are done with a digital audio interface. First, the interface is calibrated with a digital oscilloscope. The output gain was altered until a sine wave with a digital amplitude of ± 1 corresponded to a voltage of ± 1 V at the output of the interface.

As Fig. 4 illustrates, Output 1 of the interface is connected to the input of the guitar amplifier under test and the output of the amplifier is connected to a power attenuator, which matches the impedance of the amplifier output and provides a line-out, which is connected to input 1 of the audio interface. The direct connection is used to design a compensation filter, described in [12], which reduces the influence of the audio interface when measuring frequency responses with sine sweeps. The recorded direct signal is also used as the input signal for the digital model. This is advantageous because the measured direct signal is automatically synchronized in time with the amplifier output, a crucial requirement for the following iterative optimization.

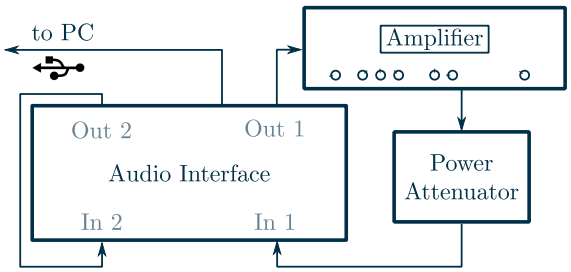

Figure 4: *Measurement Setup.*

The used power attenuator was, unfortunately, purely resistive. A reactive power attenuator would be preferable because the amplifier might constitute a resonant behavior for certain frequencies, which does not occur with a purely resistive load.

4. SYSTEM IDENTIFICATION

This section describes the steps needed to adapt the digital model to a reference system. The process is subdivided into several steps to assure that the iterative optimization does not converge into a local minimum. At first the linear part of the reference system is measured and afterwards the parameters of the nonlinear blocks are optimized.

4.1. Filters

The method used in this work to measure the linear part of the reference system is the same as described in [6]. An exponential sine sweep is sent through the reference device and the recorded output is convolved with an inverse filter. The resulting impulse response contains the linear impulse response as well as different impulse reponses for higher order harmonics. In this work only the impulse response corresponding to the linear part of the circuit is used.

To adapt the filters of the model several steps are used. First the small signal impulse response is measured with an exponential sine sweep from 10 Hz to 21 kHz and an amplitude of 0.01 V. This yields the filter $h_{\text{low}}(n)$. Afterwards the same measurement is repeated, but with an amplitude of 1 V, resulting in $h_{\text{high}}(n)$.

The low amplitude sweep is not exposed to the nonlinear behavior of the reference system and contains the influence of all its' filters. The high amplitude sine sweep gets distorted and the influence of some of the reference systems' filters is removed by the nonlinear parts of the reference system. This behavior is depicted in Fig. 5. The preceding filter $H(z)$ alters the amplitude of a sine wave which then passes through a nonlinear 'block' and is amplified back to the maximum amplitude, thus negating the influence of the preceding filter. The high amplitude sweep gets distorted and contains the influence of the last filter of the reference system. The obtained impulse responses are transformed into frequency-

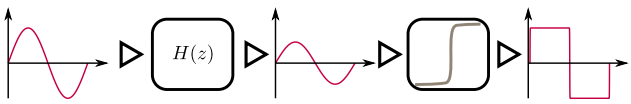

Figure 5: *Influence of filters and nonlinear blocks.*

domain with a discrete Fourier transform using 16384 samples to have a high frequency resolution. Afterwards, the small signal frequency response is divided by the large signal frequency response,

$$H_1(k) = \frac{H_{\text{low}}(k)}{H_{\text{high}}(k)}. \tag{3}$$

The resulting filter is transformed back into time-domain and used as the input filter of the digital model. The output is filtered with the measured impulse response of the high amplitude sweep $h_3(n) = h_{\text{high}}(n)$.

The results of this method are not perfect. The filters may be partially misidentified, because the gain of the last nonlinearity in the signal chain might not be high enough to negate the influence of the preceding filters. For this reason a 256 tap finite impulse response (FIR) filter $H_2(z)$ is adapted to match the small signal frequency response of the reference device. The FIR filter is located between the nonlinear blocks of the model.

The parameters for the linear part of the model are the FIR filters coefficients. The input signal for the adaptation is the above mentioned low amplitude sine sweep. The cost function calculates the difference of the magnitude spectrum of reference system and digital model output and the filter coefficients are adjusted to minimize the error between both spectra.

The length of the filter is a trade-off between computational complexity during optimization and frequency resolution and was

chosen empirically. The optimization algorithm approximates the derivative of the model output with respect to each parameter (in this case the 256 coefficients) using finite differences, leading to time-consuming calculations.

4.2. Nonlinear Blocks

After the small signal frequency response has been adapted, the filter coefficients of the FIR filter are not changed anymore, only the parameters of the nonlinear blocks can be altered.

Each nonlinear block features a multiplication with a variable gain (pre- and post-gain) of input signal and output signal. The intensity of the bias-point shift mentioned in Section 2.1 is adaptable for each nonlinear block, as well as the 'blend' stage, where dry and wet signal can be mixed by an adaptable parameter.

The first nonlinear block of the digital model also uses the parameters mentioned in Section 2.1. To limit the number of parameters, only the first 40 overtones $k_0 - k_{40}$ can be adapted. The optimization routine only alters the k_n parameters from which the polynomial coefficients a_n are computed. If the polynomial coefficients are used as parameters, too many unsuitable (or unstable) solutions would be possible and the optimization routine would not converge. The typical fundamental frequency region of an electric guitar in standard tuning ranges from $80\,\text{Hz}$ to $1100\,\text{Hz}$, depending on the number of frets. 40 harmonics do not cover the whole frequency region for the tones with the lowest pitch, but usually the contribution to the overall spectrum of the 40^{th} harmonic is negligible.

The nonlinear parameters are adapted for different input signals (of different complexity) and with different cost functions to assure convergence of the parameters into their global minimum. The used algorithm is always the Levenberg–Marquardt optimization routine, as described in [9] with different cost functions.

- At first, a grid search for the pre- and post-gain of the power-amplifier nonlinearity is performed because these parameters have the most influence on the shape of the output envelope of the digital model. The cost function calculates the difference of the envelopes of the output signals and the gain combination with the lowest error is chosen. The envelope is calculated by low-pass filtering the absolute value of the signal. The cut-off frequency of the used low-pass filter is $f_c = 10\,\text{Hz}$.
- Afterwards all nonlinear parameters are adapted at the same time. The cost function, however, was designed differently in this optimization step. It calculates the sum of squares between digital model and reference system,

$$C(\mathbf{p}) = (y(n) - \hat{y}(n, \mathbf{p}))^2, \tag{4}$$

  with $y(n)$ as the (digitized) output of the reference system and $\hat{y}(n, \mathbf{p})$ as the output of the digital model. $\mathbf{p}$ is the parameter vector of the digital model. In this optimization step, all filters except the input filter H_1 are turned off during optimization. The chosen input signal is a $1000\,\text{Hz}$ sine wave with amplitudes from $1\,\text{V}$ down to $0.001\,\text{V}$. This first step helps to find a set of parameters which can be used as initial parameters in the next optimization step where all filters in the digital model are turned back on.
- The next optimization step is done with a multi-frequency sine wave. The phase shift between each frequency is chosen in such a way that the peak-factor of the sum of the different frequencies is minimal and the signal has a flat power-spectrum [13]. The cost function in this case calculates the linear spectrogram of both signals and only compares the magnitude spectrogram, disregarding the phases. The spectrogram is initially calculated with the Fourier transform, but the frequency bins are merged into a semitone-spectrum, starting from $f_0 = 27.5\,\text{Hz}$. Additionally the magnitude spectrogram is weighted with the inverted absolute threshold of hearing. Afterwards both spectrograms are subtracted from another and all values are squared and summed up to calculate the error value.
- For guitar amplifiers with nonlinear behavior it has been beneficial to add a last step, where the same cost function (spectrogram) is used but a recorded guitar track is used as input, which consists of a combination of guitar tones and chords to further refine the parameters of the digital model.

5. RESULTS

Evaluating the quality of the adapted model is not a trivial task. There are very few perceptually motivated objective scores and they are neither suited for virtual analog modeling evaluation nor are they available for free. There exist perceptually motivated scores like PEAQ or PEMO-Q [14, 15], but they were designed for a different purpose and therefore are not suited for quality assessment of virtual analog modeling.

For this reason the adapted digital model is rated with different methods, first it is evaluated with objective measures. If these objective metrics are close to zero, the result of the modeling process is always good. But in some cases the error is relatively high, but the quality of the adapted model is quite good from a perceptual point of view. This is why a listening test was conducted to assess the quality of the adapted models perceptually. The files which were used in the listening test were also used to calculate the objective scores.

The results are evaluated for different amplifier models and for different guitar signals. Some amplifiers are tested in multiple settings, creating distortion with the pre-amplifier, the power-amplifier or both at once. Other amplifiers are tested in an artist preferred setting, where the user controls of the amplifiers are not altered from the settings the artists used in the rehearsal room.

Figure 6 shows the amplifiers in the artist preferred setting. All amplifiers produced very little distortion in the output signal. The first amplifier (top), the Ampeg VT-22, did not feature separate controls for pre-amplifier and power-amplifier and the reverb was turned off. The Fender Bassman 100 (middle) and Fender Bassman 300 (bottom) were set up to introduce almost no distortion, as can be seen by the gain and volume controls.

Different input signals are used for each amplifier. Input signals from three guitars with different pick-ups are tested:

1. single coil pick-up (SC)
2. humbucker pick-up with medium output (HM1)
3. humbucker pick-up with high output (HM2)

Only the amplifiers which were modeled in the 'artist preferred' setting, were set up to have a clean sound, introducing very little distortion in the output signal. The amplifiers which introduced a lot of distortion in the output signal were modeled in multiple settings:

1. High gain and low volume (pre-amp distortion)

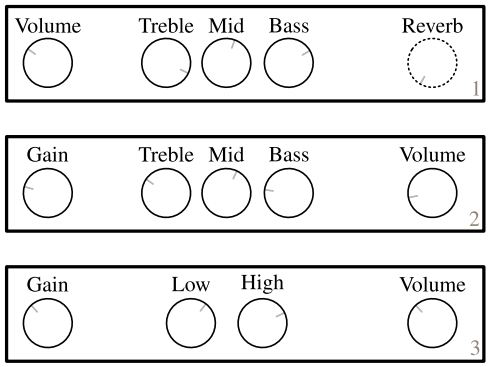

Figure 6: *Settings for amplifiers in clean setting. 1.) Ampeg VT-22 (top) 2.) Fender Bassman 100 (middle) 3.) Fender Bassman 300 (bottom)*

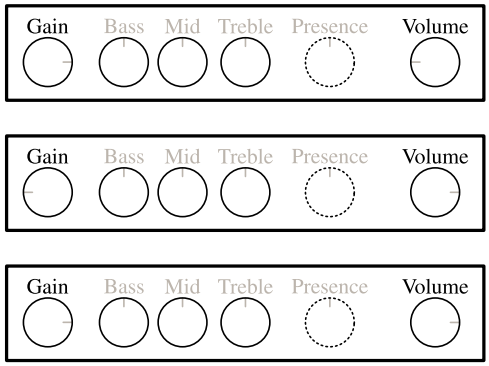

Figure 7: *Settings for pre-amp distortion (top), power-amp distortion (middle) and heavy distortion (bottom).*

2. Low gain and high volume (power-amp distortion)
3. high gain and high volume (heavy distortion)

These settings are illustrated in Fig. 7. The tone-section of the amplifiers were set to 12 o'clock and the presence knob is depicted with a dashed line, because only the Marshall - JCM 900 featured a presence control.

5.1. Objective Scores

Two scores are used to evaluate how well the model was adapted. The 'error to signal ratio' and the correlation coefficient. The error to signal ratio is defined as the energy of the time-domain error between reference device and digital model,

$$ESR = \frac{\sum_{n=-\infty}^{\infty} (y(n) - \hat{y}(n, \mathbf{p}))}{\sum_{n=-\infty}^{\infty} y(n)}. \quad (5)$$

The correlation coefficient describes the linear dependence of two random variables. In this case $y(n)$ and $\hat{y}(n, \mathbf{p})$ are considered as random variables and the correlation coefficient is calculated according to,

$$\rho(y(n), \hat{y}(n, \mathbf{p})) = \frac{\text{cov}(y(n), \hat{y}(n, \mathbf{p}))}{\sigma_{y(n)} \sigma_{\hat{y}(n, \mathbf{p})}}. \quad (6)$$

Fender Bassman 100 (Blackface-Mod)	**ESR**	ρ
Single coil (SC)	0.0412	0.9795
Humbucker medium (HM1)	0.0779	0.9611
Humbucker high (HM2)	0.0518	0.9752

Table 1: *Objective scores for the Bassman 100 with no distortion.*

Ampeg VT-22	**ESR**	ρ
Single coil (SC)	0.0745	0.9631
Humbucker medium (HM1)	0.1170	0.9417
Humbucker high (HM2)	0.1742	0.9127

Table 2: *Objective scores for the VT-22 with very little distortion.*

The results in Tabs. 1 and 2 show that the proposed method works very well with clean or almost clean amplifiers. For the Bassman 100 the ESR remains below 0.1 and the correlation coefficient never drops below 0.96.

The VT-22 also gives very good results, but when the input signal level is high, the error becomes higher too. This can be seen from the results in Tab. 2, where the ESR gets worse if the guitar input has a higher voltage. For the single coil guitar input the ESR is 0.0745 but if the input voltage is higher, which leads to more distortion, the ESR gets above 0.1. The correlation coefficient has the same tendency as the ESR.

Any reference device can add distortion either by increasing the gain, which leads to a clipping pre-amplification stage or by increasing the volume, which leads to a clipping power-amplification stage. The power-amplifier in the reference device is rarely turned up to high values, because it reaches very high sound pressure levels, when the amplifier is connected to a speaker [16], but while measuring only a dummy-load was connected to the reference device.

The results of the modeling process are shown in Tab. 3. Due to the nonlinear behavior of the reference device, the error does not increase proportionally with a rising input level and is already quite high.

Usually a guitarist will add distortion by increasing the gain knob on the amplifier. When comparing the same reference device with a clipping power-amplifier to a clipping pre-amplifier the objective error scores nearly double (see Tab. 4). But this impression is not reflected in the perceived difference between digital model and reference device.

Finally, the objective scores for the reference amplifier which introduced the most distortion in the output signal are shown in Tab. 5. In this case, the error energy is always higher than the actual signal energy, since the ESR is always greater than 1 for all test items. This is also the model which has the greatest deviation from the reference device from a perceptual point of view.

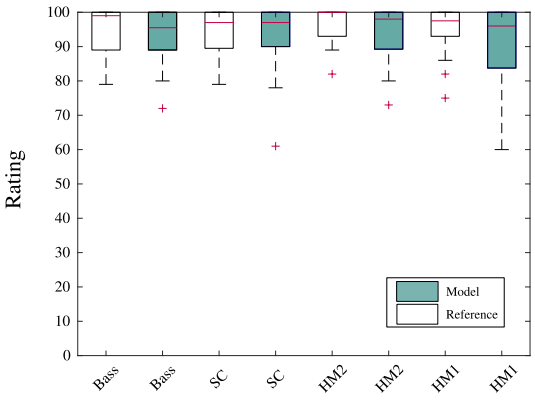

(a) *Fender Bassman 100 (clean setting).*

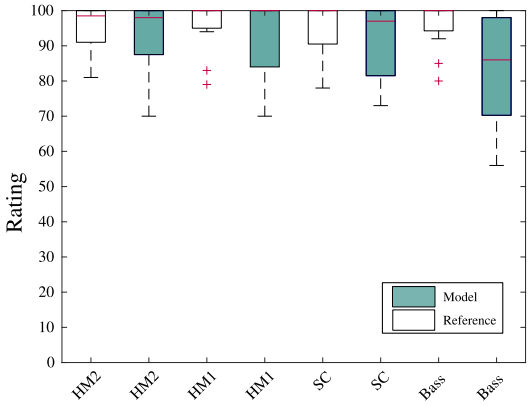

(b) *Ampeg VT-22 (clean setting).*

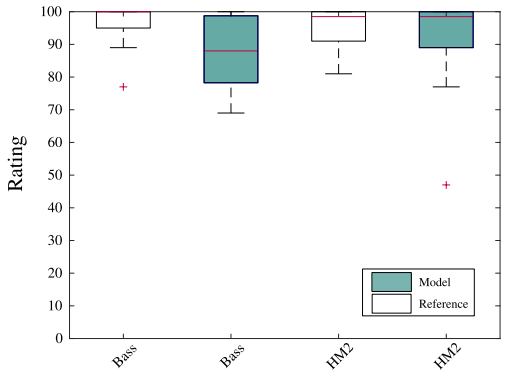

(c) *Fender Bassman 300 (clean setting).*

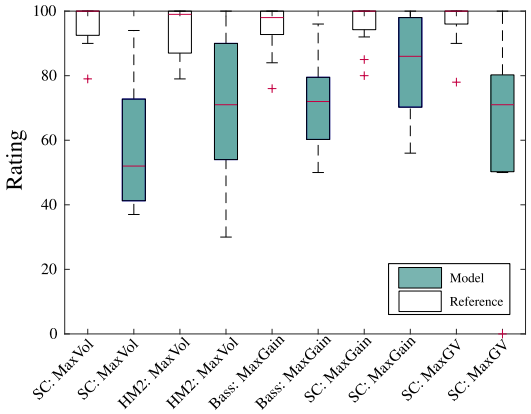

(d) *Madamp A15Mk2 with different distortion settings.*

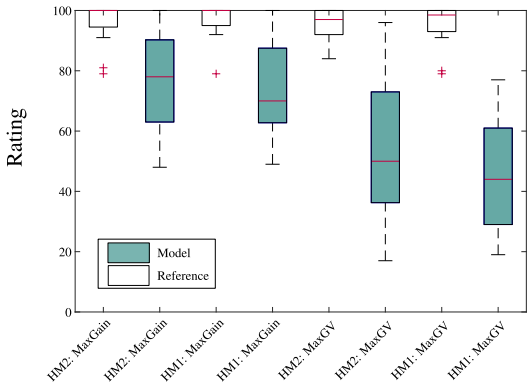

(e) *Marshall JCM900 with different distortion settings.*

Figure 8: *Results of the listening test for all tested amplifiers.*

5.2. Listening Test

A listening test was conducted to see how well the adapted models perform for a human test subject. The listening test aimed at rating the adapted model in relation to the analog reference device. The test subjects were presented with a reference item and two test items. The items should be rated according to how **similar** they sound to the reference, where 100 represents no detectable difference between the item and the reference and 0 represents a very annoying difference. One of the test items was a hidden reference, which was the same audio-file as the reference item.

The listening test featured 20 listening examples with hidden reference and digital model output and is currently still ongoing. So far 15 participants have taken the test from which 8 were ex-

Madamp A15Mk2	**ESR**	ρ
Single coil (SC)	0.4372	0.7762
Humbucker medium (HM1)	0.3709	0.8104
Humbucker high (HM2)	0.3145	0.8393

Table 3: *Objective scores for the A15Mk2 with power-amp distortion (low gain, high volume).*

Madamp A15Mk2	**ESR**	ρ
Single coil (SC)	0.8727	0.5383
Humbucker medium (HM1)	0.6596	0.6552
Humbucker high (HM2)	0.8236	0.5570

Table 4: *Objective scores for the A15Mk2 with pre-amplifier distortion (high gain, low volume).*

Marshall JCM900	**ESR**	ρ
Single coil (SC)	1.5277	0.4603
Humbucker medium (HM1)	1.5022	0.2486
Humbucker high (HM2)	1.5488	0.2237

Table 5: *Objective scores for the JCM900 with maximum distortion (high gain, high volume).*

perienced listeners, 4 were musicians and 2 were unexperienced listeners. At the end of the test, each participant had the option to comment on the test. The framework for the listening test was the 'BeaqleJS' framework, described in [17]. It features example configurations for ABX and Mushra style listening tests. The Mushra configuration was adapted to fit the needs for model – reference comparison.

The test results have been cleaned by deleting the ratings where the hidden reference was rated with a score lower than 75, but only one test subject was removed from the evaluation completely, because for 13 of 20 items, the hidden reference was rated with scores much lower than 75. Figures 8a – 8e show the results of the listening test. The bar displays the 50% quantile (median) for each item. The lower and upper bounds of the box represent the 25% quantile or the 75% quantile respectively. Outliers are depicted as crosses.

Figures 8a and 8b show the results for the reference amplifiers in clean setting and the adapted models. The results show that the digital model is always rated in the same range as the analog reference device for the test items 'Bass', 'Single Coil (SC)', 'Humbucker 1 (HM1)' and 'Humbucker 2 (HM2)'. These results confirm that the model is very well adapted as the objective scores, mentioned in Section 5.1, suggest.

The results for the Ampeg VT-22 are similar to the results of the Fender Bassman 100. In some cases there was an unwanted 'crackling' noise in the recording of the reference amplifier, which was not reproduced by the digital model. This made it possible to identify the difference between the hidden reference and the digital model output.

The last amplifier which is in an almost clean setting was the Fender Bassman 300 (Fig. 8c). Nevertheless, the HM2 (humbucker with high output voltage) test item had a nearly identical rating as the hidden reference. Only for the input signal from an electric-bass, there were minor audible differences in the output signal. These results are in agreement with the comments from the participants. Several stated, that they could not perceive any difference when the amps were in a 'clean' or 'almost clean' setting.

The results of the optimization routine for distorted reference amplifiers are not as good as the results for the clean ones. The more nonlinear the amplifier becomes (more distortion), the higher is the perceivable difference between digital model and analog reference device. This assumption was already made, based on the objective scores from Section 5.1, but is confirmed by the results of the listening test.

The clipping power-amplifier of the Madamp A15Mk2 is rated worse than the clipping pre-amplifier, as shown by the single-coil (SC) items in Fig. 8d. This does not agree with the objective scores, since the error energy for the clipping power-amplifier is twice as low as the error energy for the clipping pre-amplifier. In the listening test, the clipping pre-amplifier was rated with ≈ 90 (median) and the clipping power-amplifier with ≈ 50 (median), in comparison with the hidden reference, which had a median of 100 in both cases. This suggests that these objective scores are not suitable for modeling amplifiers with a lot of distortion and a psychoacoustically motivated cost-function would drastically improve the virtual analog modeling results for distorted amplifiers.

The listening test results for the last amplifier confirm the assumption, that a reference device with high nonlinear behavior is not identified as well as a system with little nonlinear behavior. The Marshall JCM 900 was rated worse if both pre- and power-amplifier were at high values, in comparison to the first 2 test items were only the pre-amplifier was set to a high value. A common comment from the participants was, that a difference in the noise floor between digital model and reference device made it possible to distinguish the reference from the model.

6. CONCLUSION

This work presents an approach for modeling guitar amplifiers with system identification methods. Input – output measurements are made on a reference device and a digital model, consisting of filters and nonlinear mapping functions, is adapted to recreate the characteristics of the reference device. The results showed that this method performs very good for reference amplifiers in a clean setting with almost no harmonics. If the amplifier introduces distortion, the modeling process does not perform as well.

It is possible to tune the digital model by hand, although it is not recommended. This is an indication that the model is able to recreate also highly nonlinear systems. Therefore a psychoacoustically motivated cost-function for the iterative optimization routine needs to be developed to improve the results for highly nonlinear systems.

All signals were recorded while the amplifier was not connected to a cabinet. The influence of a cabinet could lead to reduced high frequency content in the output signal, which could lessen the perceived difference between reference device and digital model.

The amplitude of the sine sweep to measure the small signal frequency response of the reference device was set to 0.01 V, which might be too high for some amplifiers and lead to a distorted output. This was not the case for the tested amplifiers but to ensure a correct modeling result a total harmonic distortion measurement should be performed and the amplitude of the sweep should be adapted accordingly to avoid faulty measurements.

7. REFERENCES

[1] David Te-Mao Yeh, *Digital implementation of musical distortion circuits by analysis and simulation*, Ph.D. thesis, Stanford University, 2009.

[2] J. Macak, *Real-time Digital Simulation of Guitar Amplifiers as Audio Effects*, Ph.D. thesis, Brno University of Technology, 2011.

[3] K. Dempwolf, *Modellierung analoger Gitarrenverstärker mit digitaler Signalverarbeitung*, Ph.D. thesis, Helmut-Schmidt-University, 2012.

[4] K.J. Werner, J.O. Smith, and J.S. Abel, "Wave digital filter adaptors for arbitrary topologies and multiport linear elements," in *Proc. Digital Audio Effects (DAFx-15)*, Trondheim, Norway, Nov. 30 - Dec. 3 2015.

[5] W. R. Dunkel, M. Rest, K. J. Werner, M. J. Olsen, and J. O. Smith III, "The fender bassman 5f6-a family of preamplifier circuits – a wave digital filter case study," in *Proc. Digital Audio Effects.(DAFx-16)*, Brno, Czech Republic, Sept. 2016.

[6] A Novak, L. Simon, P. Lotton, and J. Gilbert, "Chebyshev model and synchronized swept sine method in nonlinear audio effect modeling," in *Proc. Digital Audio Effects (DAFx-10)*, Graz, Austria, Sept. 6-10, 2010.

[7] Fractal Audio Systems, "Multipoint Iterative Matching and Impedance Correction Technology (MIMIC)," Tech. Rep., Fractal Audio Systems, April 2013.

[8] C. Kemper, "Musical instrument with acoustic transducer," June 12 2008, US Patent App. 11/881,818.

[9] F. Eichas and U. Zölzer, "Black-box modeling of distortion circuits with block-oriented models," in *Proc. Digital Audio Effects (DAFx-15)*, Trondheim, Norway, Nov 30 – Dec 3 2015.

[10] J. Pakarinen and D.T. Yeh, "A review of digital techniques for modeling vacuum-tube guitar amplifiers," *Computer Music Journal*, vol. 33, no. 2, pp. 85–100, 2009.

[11] F. Eichas, S. Mölller, and U. Zölzer, "Block-oriented modeling of distortion audio effects using iterative minimization," in *Proc. Digital Audio Effects (DAFx-15)*, Trondheim, Norway, Nov 30 – Dec 3 2015.

[12] A. Farina, "Advancements in impulse response measurements by sine sweeps," in *Audio Engineering Society Convention 122*. Audio Engineering Society, 2007.

[13] M. Schroeder, "Synthesis of low-peak-factor signals and binary sequences with low autocorrelation (corresp.)," *IEEE Transactions on Information Theory*, vol. 16, no. 1, pp. 85–89, 1970.

[14] International Telecommunication Union, "Bs.1387: Method for objective measurements of perceived audio quality," Available online at `http://www.itu.int/rec/R-REC-BS.1387` — accessed April 4th 2017.

[15] Rainer Huber and Birger Kollmeier, "Pemo - q – a new method for objective audio quality assessment using a model of auditory perception," *IEEE Transactions on audio, speech, and language processing*, vol. 14, no. 6, pp. 1902–1911, 2006.

[16] M. Zollner, "Die dummy-load als lautsprecher ersatz (the dummy-load as speaker replacement)," in *GITEC Forum*, 2016.

[17] S. Kraft and U. Zölzer, "Beaqlejs: Html5 and javascript based framework for the subjective evaluation of audio quality," in *Linux Audio Conference, Karlsruhe, DE*, 2014.